Aalto University

Aaltodoc

OPEN ACCESS

This is an electronic reprint of the original article.
This reprint may differ from the original in pagination and typographic detail.

Author(s): Qu, Zengcai & Tuovinen, Toni & Hinkkanen, Marko

Title: Inclusion of magnetic saturation in dynamic models of synchronous reluctance motors

Year: 2012

Version: Post print

Please cite the original version:

Inclusion of Magnetic Saturation in Dynamic Models of Synchronous Reluctance Motors

Zengcai Qu, Toni Tuovinen, and Marko Hinkkanen

Aalto University School of Electrical Engineering
P.O. Box 13000, FI-00076 Aalto, Finland

Abstract—**This paper deals with the modeling of the magnetic saturation in synchronous reluctance motors (SyRMs). The saturation is modeled by means of analytical expressions, which can be easily embedded in dynamic equivalent-circuit models. A modified power function—proposed in this paper—can take into account the cross saturation between the orthogonal windings, it is physically consistent, and the number of its parameters is small. The function can be used in real-time control applications and in computer simulations. The model fits well to the experimentally measured inductances of a 6.7-kW SyRM. As an application example, the proposed saturation model was implemented in a full-order observer of a motion-sensorless drive, and experimental results are shown.**

Index Terms—**Cross saturation, efficiency optimization, inductances, reciprocity conditions, synchronous reluctance motor.**

I. Introduction

The synchronous reluctance motor (SyRM) is becoming an important alternative in vector-controlled drives. In addition to its simple and robust structure, advantages of modern transverse-laminated SyRMs compared to other AC motors are [1], [2]:

1) Absense of the rotor winding results in higher efficiency and higher temperature capacity (i.e., higher rated torque for a given frame size) than in the induction motor.
2) Lower production cost compared to the permanent-magnet synchronous motor. High-speed operation and flux-weakening control can be easily achieved because of no magnets in the rotor.
3) Typically lower torque ripple, vibration, and noise compared to the switched reluctance motor.

These benefits attract industry and academia, but there are still issues to be considered in SyRMs, one of them being the modeling of the magnetic saturation.

The SyRMs are often operated with extreme saturation to achieve high torque density, and the inductances vary as a function of the currents (or fluxes). The cross-saturation of the inductances is also significant [3], [4]. Therefore, a saturation model is necessary in many applications, such as motion-sensorless control and efficiency optimization.

In control algorithms, the magnetic saturation can be taken into account via look-up tables, online parameter estimation [5], [6], [7], or explicit functions [8], [4]. The look-up table is a simple way to model the saturation characteristics, but it needs a large amount of measurement data and memory. Furthermore, the look-up table is discontinuous and defined only in the measurement range, and the interpolation may

not be very efficient. The dynamic performance of the online inductance estimation can be insufficient, and the inductance estimation may require additional excitation signal in sensorless drives. The inductances can be calculated offline using a finite-element method, if the geometry of the machine and the material properties are known [9]. However, finite-element methods cannot be used in real-time control because they are computationally very demanding.

In real-time applications, explicit continuous functions are preferable for several reasons: (i) no need to store the measured inductances; (ii) continuous and differentiable; and (iii) available in sufficient range. Furthermore, they are convenient in numerical analyses and computer simulations. In this paper, dynamic models of the SyRM are described in Section II, and explicit functions for modeling the magnetic saturation are reviewed in Section III. A saturation model using explicit power functions is proposed in Section IV. The proposed function can take the cross-saturation into account and the number of its parameters is small. As shown in Section V, the model fits well to the measured inductances of a 6.7-kW SyRM. Further, the proposed saturation model is experimentally demonstrated in a motion-sensorless SyRM drive.

II. SyRM Model

The dynamic model of the SyRM is briefly described in the following, taking into account the nonlinearity due to the magnetic saturation. The saturation can be modeled as a function of the flux or as a function of the current. In order to formulate a nonlinear state equation, the state variable should agree with the independent variable of the saturation model. This selection of the state variable affects the complexity of the whole dynamic model.

The d-axis of the rotating coordinate system is defined as the direction of the maximum inductance. Real space vectors will be used in the model. For example, the stator-current vector is $\boldsymbol{i}_s = [i_d, i_q]^T$, where i_d and i_q are the components of the vector and the matrix transpose is marked with the superscript T. The magnitude is denoted by

$$i_s = \sqrt{i_d^2 + i_q^2} \qquad (1)$$

The orthogonal rotation matrix is $\mathbf{J} = \begin{bmatrix} 0 & -1 \\ 1 & 0 \end{bmatrix}$. Per-unit quantities will be used.
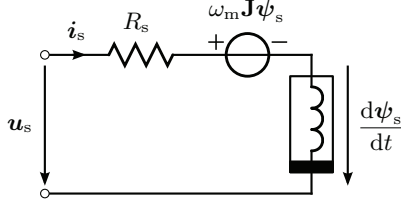
Fig. 1. Dynamic space-vector model in rotor coordinates. The nonlinear inductor can be defined either by $\boldsymbol{i}_\mathrm{s} = \boldsymbol{i}_\mathrm{s}(\boldsymbol{\psi}_\mathrm{s})$ or $\boldsymbol{\psi}_\mathrm{s} = \boldsymbol{\psi}_\mathrm{s}(\boldsymbol{i}_\mathrm{s})$.

A. Flux as a State Variable

The dynamic equivalent circuit in rotor coordinates is illustrated in Fig. 1. The stator-voltage equation is

$$\frac{\mathrm{d}\boldsymbol{\psi}_\mathrm{s}}{\mathrm{d}t} = \boldsymbol{u}_\mathrm{s} - R_\mathrm{s}\boldsymbol{i}_\mathrm{s} - \omega_\mathrm{m}\mathbf{J}\boldsymbol{\psi}_\mathrm{s} \tag{2}$$

where $\boldsymbol{\psi}_\mathrm{s}$ is the stator-flux vector, $\boldsymbol{u}_\mathrm{s}$ the stator-voltage vector, R_s the stator resistance, and ω_m the electrical angular speed of the rotor. If the magnetic saturation were omitted, $i_\mathrm{d} = \psi_\mathrm{d}/L_\mathrm{d}$ and $i_\mathrm{q} = \psi_\mathrm{q}/L_\mathrm{q}$ would hold. However, due to the magnetic saturation, the components of the stator-current vector become nonlinear functions of the flux components[1]

$$\boldsymbol{i}_\mathrm{s} = \boldsymbol{i}_\mathrm{s}(\boldsymbol{\psi}_\mathrm{s}) = \begin{bmatrix} i_\mathrm{d}(\psi_\mathrm{d}, \psi_\mathrm{q}) \\ i_\mathrm{q}(\psi_\mathrm{d}, \psi_\mathrm{q}) \end{bmatrix} \tag{3}$$

A nonlinear state-space representation is obtained by substituting (3) into (2). The signal-flow graph of the model is shown in Fig. 2(a). Fig. 3 illustrates an example of saturation characteristics.

The power balance of the SyRM model is given by

$$\boldsymbol{u}_\mathrm{s}^\mathrm{T}\boldsymbol{i}_\mathrm{s} = R_\mathrm{s}i_\mathrm{s}^2 + \frac{\mathrm{d}W_\mathrm{f}}{\mathrm{d}t} + T_\mathrm{e}\omega_\mathrm{m} \tag{4}$$

where the electromagnetic torque is

$$T_\mathrm{e} = \boldsymbol{i}_\mathrm{s}^\mathrm{T}\mathbf{J}\boldsymbol{\psi}_\mathrm{s} = i_\mathrm{q}\psi_\mathrm{d} - i_\mathrm{d}\psi_\mathrm{q} \tag{5}$$

and the rate of change of the magnetic energy is

$$\frac{\mathrm{d}W_\mathrm{f}}{\mathrm{d}t} = \boldsymbol{i}_\mathrm{s}^\mathrm{T}\frac{\mathrm{d}\boldsymbol{\psi}_\mathrm{s}}{\mathrm{d}t} = i_\mathrm{d}\frac{\mathrm{d}\psi_\mathrm{d}}{\mathrm{d}t} + i_\mathrm{q}\frac{\mathrm{d}\psi_\mathrm{q}}{\mathrm{d}t} \tag{6}$$

It is worth noticing that the current components i_d and i_q are functions of the flux components according to (3). If needed, the core losses can be modeled separately, and the nonlinear inductor should not generate or dissipate electrical energy. The conservation of energy leads to the reciprocity condition [10], [11], [3]:

$$\frac{\partial i_\mathrm{d}(\psi_\mathrm{d}, \psi_\mathrm{q})}{\partial \psi_\mathrm{q}} = \frac{\partial i_\mathrm{q}(\psi_\mathrm{d}, \psi_\mathrm{q})}{\partial \psi_\mathrm{d}} \tag{7}$$

[1]If desired, the nonlinear functions can be represented by means of inductance functions as $i_\mathrm{d}(\psi_\mathrm{d}, \psi_\mathrm{q}) = \psi_\mathrm{d}/L_\mathrm{d}(\psi_\mathrm{d}, \psi_\mathrm{q})$ and $i_\mathrm{q}(\psi_\mathrm{d}, \psi_\mathrm{q}) = \psi_\mathrm{q}/L_\mathrm{q}(\psi_\mathrm{d}, \psi_\mathrm{q})$. In the latter part of the paper, both forms will be used.
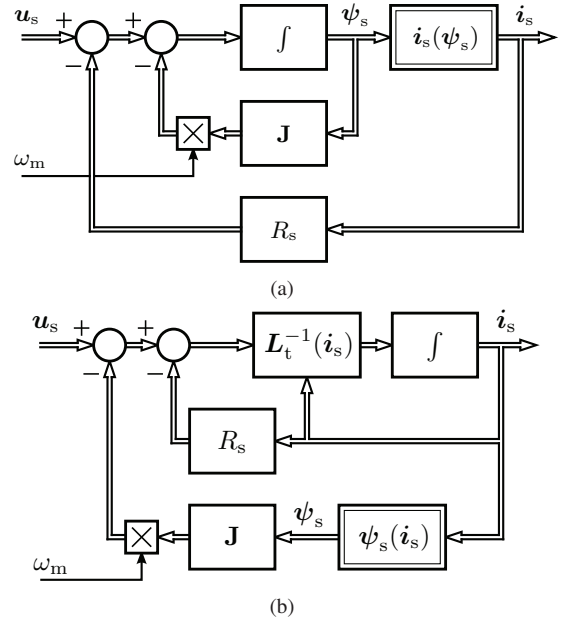

(a)

(b)

Fig. 2. Signal-flow graph of the saturable SyRM model: (a) stator flux as a state variable; (b) stator current as a state variable.
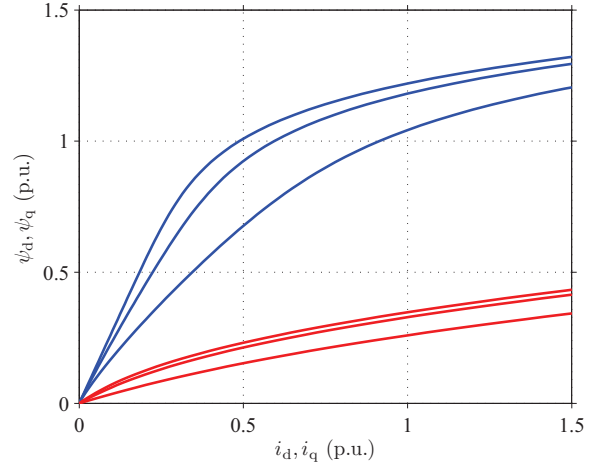

Fig. 3. Fluxes ψ_d (blue) and ψ_q (red) as a function of i_d and i_q, respectively. The parameter of ψ_d is $i_\mathrm{q} = \{0, 0.6, 1.2\}$ p.u. and the parameter of ψ_q is $i_\mathrm{d} = \{0, 0.3, 0.6\}$ p.u.

B. Current as a State Variable

Instead of (3), the saturation can be modeled using the current components as independent variables:

$$\boldsymbol{\psi}_\mathrm{s} = \boldsymbol{\psi}_\mathrm{s}(\boldsymbol{i}_\mathrm{s}) = \begin{bmatrix} \psi_\mathrm{d}(i_\mathrm{d}, i_\mathrm{q}) \\ \psi_\mathrm{q}(i_\mathrm{d}, i_\mathrm{q}) \end{bmatrix} \tag{8}$$

In this case, the voltage equation (2) cannot be directly used to form a nonlinear state equation. Using (8), the derivatives

of the stator flux components become

$$\frac{\mathrm{d}\psi_\mathrm{d}(i_\mathrm{d}, i_\mathrm{q})}{\mathrm{d}t} = \frac{\partial \psi_\mathrm{d}}{\partial i_\mathrm{d}} \frac{\mathrm{d}i_\mathrm{d}}{\mathrm{d}t} + \frac{\partial \psi_\mathrm{d}}{\partial i_\mathrm{q}} \frac{\mathrm{d}i_\mathrm{q}}{\mathrm{d}t} \qquad (9\mathrm{a})$$

$$\frac{\mathrm{d}\psi_\mathrm{q}(i_\mathrm{d}, i_\mathrm{q})}{\mathrm{d}t} = \frac{\partial \psi_\mathrm{q}}{\partial i_\mathrm{d}} \frac{\mathrm{d}i_\mathrm{d}}{\mathrm{d}t} + \frac{\partial \psi_\mathrm{q}}{\partial i_\mathrm{q}} \frac{\mathrm{d}i_\mathrm{q}}{\mathrm{d}t} \qquad (9\mathrm{b})$$

These derivatives can be expressed using the matrix notation as $\mathrm{d}\boldsymbol{\psi}_\mathrm{s}/\mathrm{d}t = \boldsymbol{L}_\mathrm{t}(\boldsymbol{i}_\mathrm{s}) \cdot \mathrm{d}\boldsymbol{i}_\mathrm{s}/\mathrm{d}t$, where

$$\boldsymbol{L}_\mathrm{t}(\boldsymbol{i}_\mathrm{s}) = \begin{bmatrix} \dfrac{\partial \psi_\mathrm{d}(i_\mathrm{d}, i_\mathrm{q})}{\partial i_\mathrm{d}} & \dfrac{\partial \psi_\mathrm{d}(i_\mathrm{d}, i_\mathrm{q})}{\partial i_\mathrm{q}} \\ \dfrac{\partial \psi_\mathrm{q}(i_\mathrm{d}, i_\mathrm{q})}{\partial i_\mathrm{d}} & \dfrac{\partial \psi_\mathrm{q}(i_\mathrm{d}, i_\mathrm{q})}{\partial i_\mathrm{q}} \end{bmatrix} \qquad (10)$$

is the incremental inductance matrix, and its elements are functions of the current components. Hence, the voltage equation (2) becomes

$$\frac{\mathrm{d}\boldsymbol{i}_\mathrm{s}}{\mathrm{d}t} = \boldsymbol{L}_\mathrm{t}^{-1} \left(\boldsymbol{u}_\mathrm{s} - R_\mathrm{s}\boldsymbol{i}_\mathrm{s} - \omega_\mathrm{m}\mathbf{J}\boldsymbol{\psi}_\mathrm{s} \right) \qquad (11)$$

A nonlinear state equation is obtained by substituting (8) and (10) into (11). The signal-flow graph of the model is shown in Fig. 2(b).

The power balance and the torque equation are naturally independent of the choice of the state variable. The reciprocity condition for the saturation model can now be formulated as

$$\frac{\partial \psi_\mathrm{d}(i_\mathrm{d}, i_\mathrm{q})}{\partial i_\mathrm{q}} = \frac{\partial \psi_\mathrm{q}(i_\mathrm{d}, i_\mathrm{q})}{\partial i_\mathrm{d}} \qquad (12)$$

i.e., the incremental inductance matrix should be symmetric.

C. Comparison of State Variable Choices

Comparing the two different nonlinear state equations of the SyRM, it is clear that using the flux as the state variable leads to simpler equations, since the incremental inductance is avoided. Hence, the model in Section II-A is preferred in the computer simulation models and various numerical analyses.

In the case of state observers, the selection of the saturation model depends on the observer structure. In full-order observers, the saturation can be modelled as $\boldsymbol{i}_\mathrm{s}(\boldsymbol{\psi}_\mathrm{s})$ since the flux estimate is available. In reduced-order observers, the saturation has to be typically modelled as $\boldsymbol{\psi}_\mathrm{s}(\boldsymbol{i}_\mathrm{s})$ using the measured stator current as the input.

If the signal injection methods are to be designed or analyzed, the incremental inductance matrix $\boldsymbol{L}_\mathrm{t}$ is typically needed. Furthermore, the current controller gains should be tuned by taking into account the incremental inductances.

III. REVIEW OF EXPLICIT FUNCTIONS FOR MODELING SATURATION

Explicit functions for saturation models are briefly reviewed. Even if some functions below have been originally proposed for non-salient machines, they can be seen as a relevant starting point for developing expressions for SyRMs.

A. Flux as Independent Variable

1) Power Function: If the cross-saturation is omitted, the magnetic saturation can be modeled by applying a power function as [8]

$$i_\mathrm{d}(\psi_\mathrm{d}) = \frac{\psi_\mathrm{d}}{L_\mathrm{du}} \left[1 + (\alpha|\psi_\mathrm{d}|)^a \right] \qquad (13)$$

where L_du is the unsaturated inductance and α and a are nonnegative constants. The exponent a determines the shape of the saturation characteristics. An interpreration for the parameter α is that the inductance is half of the unsaturated value L_du at $\psi_\mathrm{d} = 1/\alpha$. Naturally, the q-axis current $i_\mathrm{q}(\psi_\mathrm{q})$ could be modeled using the same function (with different parameters). However, the cross-saturation cannot be directly modeled using (13). It is worth noticing that (13) could be alternatively formulated as an inductance function

$$L_\mathrm{d}(\psi_\mathrm{d}) = \frac{L_\mathrm{du}}{1 + (\alpha|\psi_\mathrm{d}|)^a} \qquad (14)$$

since $L_\mathrm{d}(\psi_\mathrm{d}) = \psi_\mathrm{d}/i_\mathrm{d}(\psi_\mathrm{d})$.

2) Arctangent Function: Typically, the incremental inductance is initially constant, undergoes a transition, and finally becomes constant again. The arctangent function has similar characteristic [12]

$$\frac{\partial i_\mathrm{d}}{\partial \psi_\mathrm{d}} = \frac{2}{\pi} M_\mathrm{d} \arctan \left[\tau_\mathrm{T} \left(|\psi_\mathrm{d}| - \psi_\mathrm{T} \right) \right] + M_\mathrm{a} \qquad (15)$$

where the shape is determined by its parameters M_a, M_d, τ_T, and ψ_T. The expression for $i_\mathrm{d}(\psi_\mathrm{d})$ is obtained by integrating (15) with respect to ψ_d, cf. [12] for the lengthy closed-form expression. The expression of $i_\mathrm{q}(\psi_\mathrm{q})$ uses the same function with separate parameters. An advantage of this arctangent-based model is that the parameters have physical interpretation, leading to comparatively easy fitting procedure.[2] However, the cross-saturation is not taken into account in (15).

B. Current as Independent Variable

Expressions for $\boldsymbol{\psi}_\mathrm{s} = \boldsymbol{\psi}_\mathrm{s}(\boldsymbol{i}_\mathrm{s})$, or equivalent expressions using inductance functions, will be discussed below. However, for dynamically accurate models, also the incremental inductances in (10) are needed, if the stator current is used as a state variable.

1) Piecewise Functions: In some applications, a very simple saturation model may suffice. In [14], the d-axis inductance is

$$L_\mathrm{d}(i_\mathrm{d}) = \begin{cases} L_\mathrm{du}, & |i_\mathrm{d}| < i_\mathrm{d0} \\ L_\mathrm{du} - \delta(|i_\mathrm{d}| - i_\mathrm{d0}), & |i_\mathrm{d}| > i_\mathrm{d0} \end{cases} \qquad (16)$$

where L_du is the unsaturated inductance and i_d0 and δ are positive parameters. The inductance L_q was kept constant and the cross-saturation was ignored. Naturally, this model can be formulated as $\psi_\mathrm{d}(i_\mathrm{d}) = L_\mathrm{d}(i_\mathrm{d})i_\mathrm{d}$ and $\psi_\mathrm{q} = L_\mathrm{q}i_\mathrm{q}$. A slightly more complicated piecewise function was applied in [15], where also the cross-saturation was taken into account. Piecewise functions can simplify the mathematical expressions, but they are not differentiable on the boundary.

---

[2]A similar function has been implemented in a built-in induction machine model of a commercial circuit simulator [13].

2) Polynomial Functions: In [16], the saturation characteristics are modeled by means of polynomials as

$$L_d(i_d, i_q) = \sum_{i=0}^{n} \sum_{j=0}^{m} a_{i,j} |i_q|^i (|i_d| - i_{d0})^j \quad (17a)$$

$$L_q(i_d, i_q) = \sum_{i=0}^{n} \sum_{j=0}^{m} b_{i,j} |i_d|^i (|i_q| - i_{q0})^j \quad (17b)$$

where the parameters $a_{i,j}$ and $b_{i,j}$ are determined using the method of least squares. A higher degree results in better accuracy and smoothness but the number of coefficients is limited by the memory of controller. In the implemented model in [16], the total number of parameters in (17) was 13. In addition to (17), separate models for the incremental inductances were applied. Typically, the accuracy of polynomial models deteriorates significantly outside the range of the data, which can be a limitation in some applications.

3) Rational Functions: In [4], the saturation was modeled as

$$L_d(i_d, i_q) = L_{d0}(i_d) - L_{d1}(i_d) L_{q2}(i_q) \quad (18a)$$
$$L_q(i_d, i_q) = L_{q0}(i_q) - L_{q1}(i_q) L_{d2}(i_d) \quad (18b)$$

where L_{d0}, L_{d1}, L_{d2}, L_{q0}, L_{q1}, and L_{q2} are all expressed as rational functions. As an example, the function

$$L_{d0}(i_d) = A + \frac{B}{i_d^4 + C i_d^2 + D} \quad (19)$$

Totally 16 parameters were needed. The model seem to fit very well to the measured data. However, it does not fulfill the reciprocity condition (12), and its accuracy may deteriorate outside the range of the data.

IV. PROPOSED MODEL

In the proposed model, the flux is considered as an independent variable. The power function in (13) is used as a starting point, since it was noticed to fit well to the no-load data. The goal is to augment the power function so that the cross-saturation can be taken into account and the number of its parameters is kept small. In order to develop explicit functions, which fulfill the reciprocity condition, functions of the following form can be considered [3]:
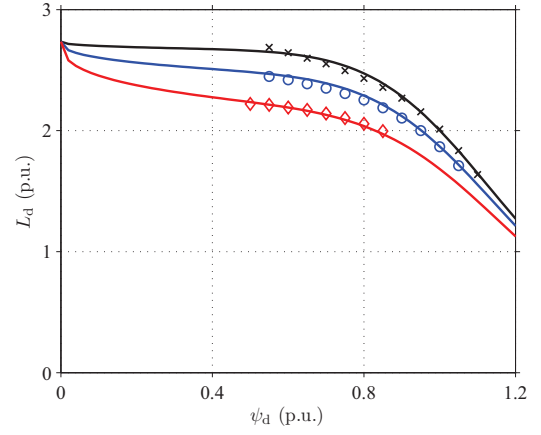
$$i_d(\psi_d, \psi_q) = i_d(\psi_d, 0) + \frac{df(\psi_d)}{d\psi_d} g(\psi_q) \quad (20a)$$

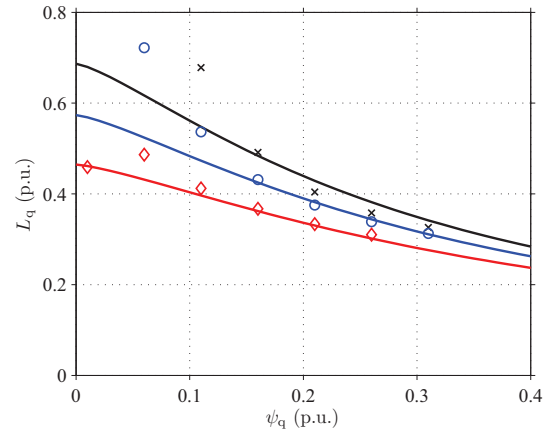$$i_q(\psi_d, \psi_q) = i_q(0, \psi_q) + f(\psi_d) \frac{dg(\psi_q)}{d\psi_q} \quad (20b)$$

where the first terms $i_d(\psi_d, 0)$ and $i_q(0, \psi_q)$ are the currents in no-load conditions. It can be easily seen that these functions fulfill (7). Augmenting the power function with $f(\psi_d) \propto \psi_d^{c+2}$ and $g(\psi_q) \propto \psi_q^{d+2}$ yields the proposed model:

$$i_d(\psi_d, \psi_q) = \frac{\psi_d}{L_{du}} \left[1 + (\alpha|\psi_d|)^a + \frac{\gamma L_{du}}{d+2} |\psi_d|^c |\psi_q|^{d+2} \right] \quad (21a)$$

$$i_q(\psi_d, \psi_q) = \frac{\psi_q}{L_{qu}} \left[1 + (\beta|\psi_q|)^b + \frac{\gamma L_{qu}}{c+2} |\psi_d|^{c+2} |\psi_q|^d \right] \quad (21b)$$

(a)

(b)

Fig. 4. Results of curve fitting to experimental data: (a) L_d as a function of ψ_d for three different values of ψ_q; (b) L_q as a function of ψ_q for three different values of ψ_d. In (a), the values of ψ_q are 0.1 p.u. (black line), 0.2 p.u. (blue line) and 0.3 p.u. (red line). In (b), the values of ψ_d are 0.6 p.u. (black line), 0.8 p.u. (blue line) and 1.0 p.u. (red line).

where L_{du} and L_{qu} are the unsaturated inductances, and α, β, γ, a, b, c, and d are nonnegative constants. The model has only nine parameters in total. A similar modeling approach has been used in connection with induction motors [17].

V. EXPERIMENTAL RESULTS

The studied motor is a transverse-laminated 6.7-kW four-pole SyRM. The rated values are: speed 3175 r/min; frequency 105.8 Hz; line-to-line rms voltage 370 V; rms current 15.5 A; and torque 20.1 Nm.

A. Data Fitting

The measurements were carried out in steady state at a constant speed $\omega_m = 0.3$ p.u. The measurement range was $i_d = 0.1 \ldots 0.7$ p.u. and $i_q = -1.4 \ldots 1.4$ p.u. The inductance data were calculated in rotor coordinates as

$$\hat{L}_d = \frac{u_q - R_s i_q}{i_d \omega_m}, \quad \hat{L}_q = \frac{u_d - R_s i_d}{i_q \omega_m} \quad (22)$$
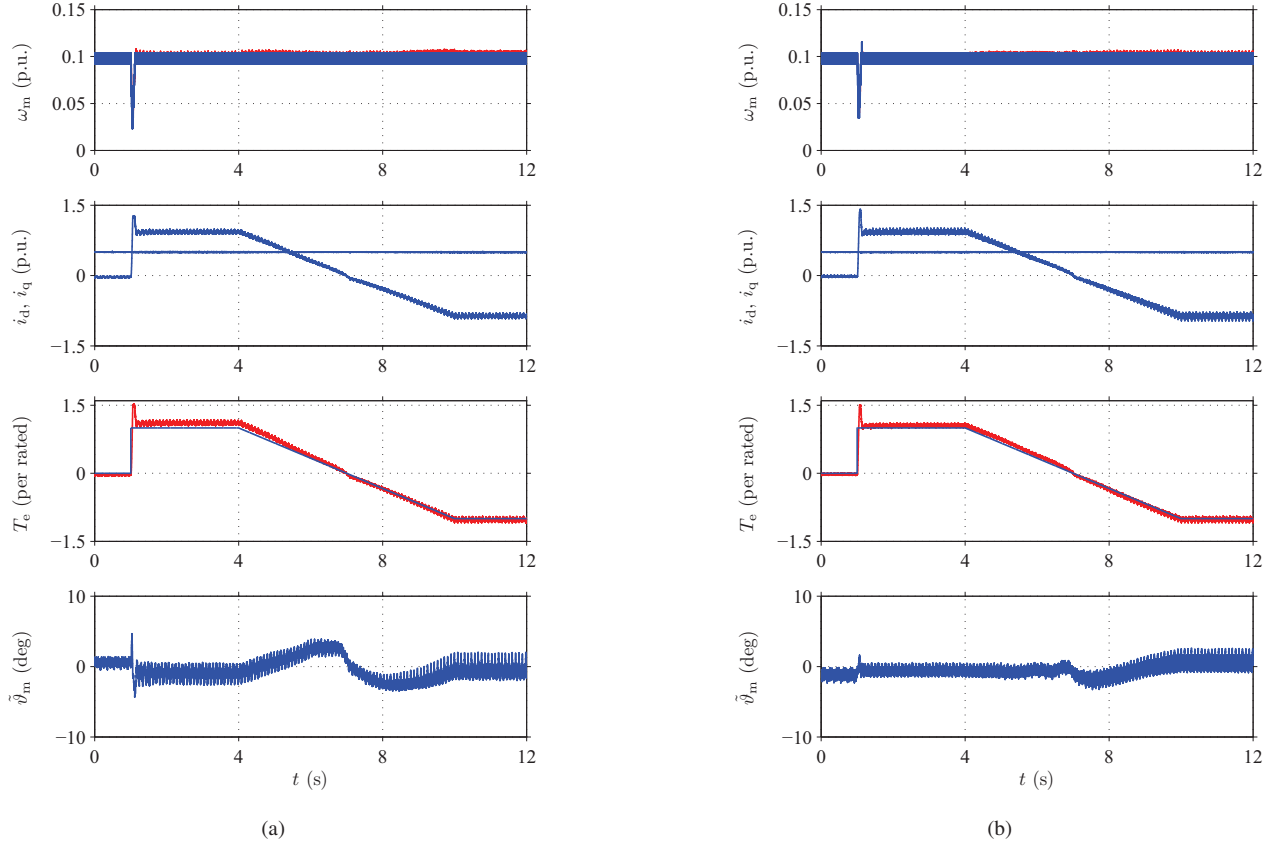
Fig. 5. Experimental results showing a slow load-torque reversal from the rated load to the negative rated load: (a) Results with constant model inductances; (b) Results with the proposed magnetic saturation model. The speed reference is 0.1 p.u. and $i_d = 0.5$ p.u. The first subplot shows the measured speed (blue) and the estimated speed (red). The second subplot shows the measured currents in the estimated rotor coordinates. The third subplot shows the torque reference of the loading drive (blue) and the estimated torque (red). The last subplot is the estimation error of the rotor position (in electrical degrees).

It is worth noticing that the inductance calculation is sensitive to small measurements errors at lowest current values.

The parameters of the proposed model are fitted by minimizing the cost function

$$
\begin{aligned}
&J(L_{du}, L_{qu}, \alpha, \beta, \gamma, a, b, c, d) \\
&= \sum_{n=1}^{N} \left(\hat{L}_{d,n} - L_{d,n} \right)^2 + \left(\hat{L}_{q,n} - L_{q,n} \right)^2
\end{aligned}
\tag{23}
$$

where the inductances L_d and L_q are calculated from the functions (21) using the actual values of the fluxes ψ_d and ψ_q in each operating point. The index n refers to an operating point and N is the total number of different operating points. Since the exponents d was noticed to approach zero in the fitting procedure, it was preset to zero. The fitted per-unit parameters are given in Table I.

The measured inductance data and the curves from the fitted functions are shown in Fig. 4. The d-axis inductance L_d is shown as a function of ψ_d for three different values of ψ_q in Fig. 4(a). Similar representation for the q-axis inductance L_q is used in Fig. 4(b). It can be seen that the proposed model fits very well to the measured data. The cross-saturation appears to be very significant in the analyzed machine; in the case of no cross-saturation, the curves in Fig. 4 would overlap.

TABLE I
FITTED PER-UNIT PARAMETERS

L_{du}	L_{qu}	α	β	γ	a	b	c	d
2.73	0.843	0.847	3.84	2.37	6.61	1.33	0.41	0

B. Application Example: Sensorless Full-Order Observer

As an application example, the proposed saturation model (21) was implemented in a full-order observer of a sensorless 6.7-kW SyRM drive [18]. The parameters given in Table I were used.

Results of changes in load torque are shown in Fig. 5. The load torque was stepped from zero to the rated value at $t = 1$ s and then reversed to the negative rated value in a ramp from $t = 4$ s to $t = 10$ s. The speed reference was kept at 0.1 p.u. Fig. 5(a) shows the results with constant model inductances and Fig. 5(b) shows the results with the proposed magnetic saturation model. It can be seen that the error in the estimated position with the proposed model is smaller at all torque levels. The slight variation in the position estimation error indicates that there are still some model uncertainties.

Results of a load-torque steps are shown in Fig. 6. The load torque was reversed from the negative rated value to the rated value at $t = 1$ s and removed at $t = 4$ s. It can be seen that the
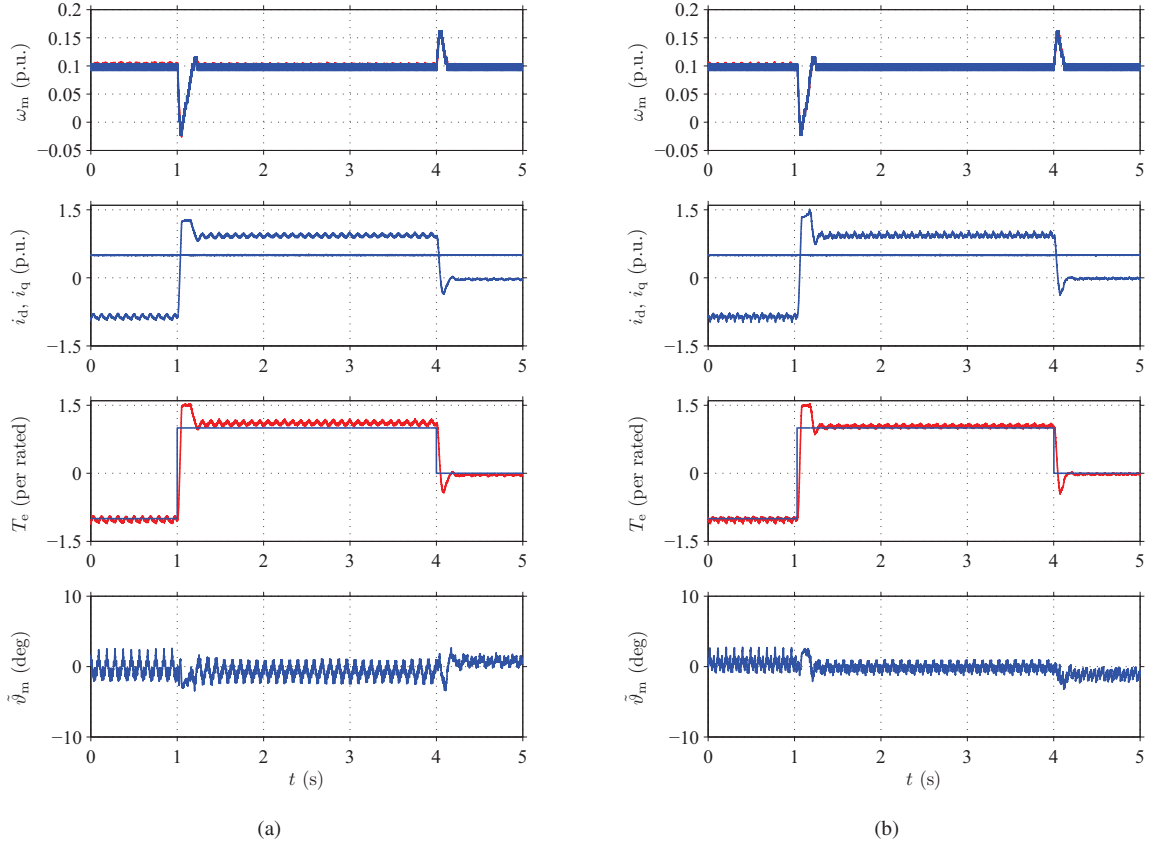
Fig. 6.   Experimental results showing load-torque steps (negative rated → rated → 0): (a) Results with constant model inductances; (b) Results with the proposed magnetic saturation model. The speed reference is 0.1 p.u. and $i_d = 0.5$ p.u.

position estimation error in transient states with the proposed model is smaller than that of without the model.

VI. CONCLUSION

This paper proposed an explicit function for modeling the magnetic saturation of the SyRM. The saturation is modeled by means of two-dimensional power functions, where the cross-coupling between the d- and q-axes is taken into account. The proposed function fulfills the reciprocity condition. The function can be easily implemented in computer simulations and real-time control algorithms. The model was fitted to the measured inductance data of a 6.7-kW SyRM. As an application example, the proposed saturation model was implemented in a full-order observer of a motion-sensorless drive. Experimental results show that the control accuracy and position estimation accuracy are improved by taking the saturation effect into account.

ACKNOWLEDGMENT

REFERENCES

[1] A. Vagati, A. Fratta, G. Franceschini, and P. M. Rosso, "Ac motors for high-performance drives: a design-based comparison," in *Conf. Rec. IEEE-IAS Annu. Meeting*, vol. 1, Orlando, FL, Oct. 1995, pp. 725–733.

[2] A. Boglietti, A. Cavagnino, M. Pastorelli, and A. Vagati, "Experimental comparison of induction and synchronous reluctance motors performance," in *Conf. Rec. IEEE-IAS Annu. Meeting*, vol. 1, Hong Kong, Oct. 2005, pp. 474–479.

[3] A. Vagati, M. Pastorelli, F. Scapino, and G. Franceschini, "Impact of cross saturation in synchronous reluctance motors of the transverse-laminated type," *IEEE Trans. Ind. Appl.*, vol. 36, no. 4, pp. 1039–1046, Aug. 2000.

[4] S. Yamamoto, T. Ara, and K. Matsuse, "A method to calculate transient characteristics of synchronous reluctance motors considering iron loss and cross-magnetic saturation," *IEEE Trans. Ind. Appl.*, vol. 43, no. 1, pp. 47–56, Jan. 2007.

[5] H. Kim, J. Hartwig, and R. D. Lorenz, "Using on-line parameter estimation to improve efficiency of IPM machine drives," vol. 2, Cairns, Australia, Nov. 2002, pp. 815–820.

[6] T. Senjyu, K. Kinjo, N. Urasaki, and K. Uezato, "High efficiency control of synchronous reluctance motors using extended Kalman filter," *IEEE Trans. Ind. Electron.*, vol. 50, no. 4, pp. 726–732, Aug. 2003.

[7] P. Niazi, H. A. Toliyat, and A. Goodarzi, "Robust maximum torque per ampere (MTPA) control of PM-assisted SynRM for traction application," *IEEE Trans. Veh. Technol.*, vol. 56, no. 4, pp. 1538–1545, Jul. 2007.

[8] H. C. J. de Jong, "Saturation in electrical machines," in *Proc. ICEM'80*, vol. 3, Athens, Greece, Sep. 1980, pp. 1545–1552.

[9] L. Chédot and G. Friedrich, "A cross saturation model for interior permanent magnet synchronous machine. Application to a starter-generator," in *Conf. Rec. IEEE-IAS Annu. Meeting*, vol. 1, Seattle, WA, Oct. 2004, pp. 64–70.

[10] J. A. Melkebeek and J. L. Willems, "Reciprocity relations for the mutual inductances between orthogonal axis windings in saturated salient-pole machines," *IEEE Trans. Ind. Appl.*, vol. 26, no. 1, pp. 107–114, Jan./Feb. 1990.

[11] P. W. Sauer, "Constraints on saturation modeling in AC machines," *IEEE Trans. Energy Convers.*, vol. 7, no. 1, pp. 161–167, Mar. 1992.

[12] K. A. Corzine, B. T. Kuhn, S. D. Sudhoff, and H. J. Hegner, "An improved method for incorporating magnetic saturation in the q-d synchronous machine model," *IEEE Trans. Energy Convers.*, vol. 13, no. 3, pp. 270–275, Sept. 1998.

[13] Plexim GmbH, *PLECS User Manual, Version 3.2*, 2012. [Online]. Available: http://www.plexim.com/files/plecsmanual.pdf

[14] C. Mademlis, "Compensation of magnetic saturation in maximum torque to current vector controlled synchronous reluctance motor drives," *IEEE Trans. Energy Convers.*, vol. 18, no. 3, pp. 379–385, Sep. 2003.

[15] T. Tuovinen, M. Hinkkanen, and J. Luomi, "Analysis and design of a position observer with resistance adaptation for synchronous reluctance motor drives," in *Proc. IEEE ECCE'11*, Phoenix, AZ, Sep. 2011, pp. 88–95.

[16] A. Kilthau and J. M. Pacas, "Appropriate models for the control of the synchronous reluctance machine," in *Conf. Rec. IEEE-IAS Annu. Meeting*, vol. 4, Pittsburgh, PA, Oct. 2002, pp. 2289–2295.

[17] T. Tuovinen, M. Hinkkanen, and J. Luomi, "Modeling of saturation due to main and leakage flux interaction in induction machines," *IEEE Trans. Ind. Appl.*, vol. 46, no. 3, pp. 937–945, May/June 2010.

[18] ——, "A comparison of an adaptive full-order observer and a reduced-order observer for synchronous reluctance motor drives," in *Proc. IEEE SLED'11*, Nottingham, UK, Sep. 2011, pp. 118–122.

BIOGRAPHY

Zengcai Qu received the B.Sc. in electrical engineering and automation in Shanghai JiaoTong University, Shanghai, China in 2007, and the M.Sc. degree in Space Science and Technology from Lulea University of Technology, Kiruna, Sweden and Helsinki University of Technology (part of Aalto University since 2010), Espoo, Finland in 2009. Since 2009, he is currently working towards the Ph.D. degree in Aalto University, Espoo, Finland. His research interest is the control of electric drives.

Toni Tuovinen received the M.Sc. degree from the University of Helsinki, Helsinki, Finland, in 2005, and the M.Sc.(Eng.) degree from Helsinki University of Technology, Espoo, Finland, in 2009. Since 2007, he has been with the Helsinki University of Technology. He is currently a Research Scientist in the Aalto University School of Electrical Engineering, Espoo, Finland. His main research interest is the control of electric drives.

Marko Hinkkanen (M'06) received the M.Sc.(Eng.) and D.Sc.(Tech.) degrees from the Helsinki University of Technology, Espoo, Finland, in 2000 and 2004, respectively. Since 2000, he has been with the Helsinki University of Technology. He is currently an Adjunct Professor in the Aalto University School of Electrical Engineering, Espoo, Finland. His research interests include electric drives and electric machines.